Robust intensity-modulated proton therapy to reduce high linear energy transfer in organs at risk

Yu An
Department of Radiation Oncology, Mayo Clinic Hospital, Phoenix, Arizona

Jie Shan
Department of Biomedical Informatics, Arizona State University, Tempe, Arizona

Samir H. Patel, William Wong, Steven E. Schild, Xiaoning Ding, Martin Bues, and Wei Liu[a)]
Department of Radiation Oncology, Mayo Clinic Hospital, Phoenix, Arizona

(Received 6 April 2017; revised 25 September 2017; accepted for publication 26 September 2017; published 26 October 2017)

Purpose: We propose a robust treatment planning model that simultaneously considers proton range and patient setup uncertainties and reduces high linear energy transfer (LET) exposure in organs at risk (OARs) to minimize the relative biological effectiveness (RBE) dose in OARs for intensity-modulated proton therapy (IMPT). Our method could potentially reduce the unwanted damage to OARs.

Methods: We retrospectively generated plans for 10 patients including two prostate, four head and neck, and four lung cancer patients. The "worst-case robust optimization" model was applied. One additional term as a "biological surrogate (BS)" of OARs due to the high LET-related biological effects was added in the objective function. The biological surrogate was defined as the sum of the physical dose and extra biological effects caused by the dose-averaged LET. We generated nine uncertainty scenarios that considered proton range and patient setup uncertainty. Corresponding to each uncertainty scenario, LET was obtained by a fast LET calculation method developed in-house and based on Monte Carlo simulations. In each optimization iteration, the model used the worst-case BS among all scenarios and then penalized overly high BS to organs. The model was solved by an efficient algorithm (limited-memory Broyden–Fletcher–Goldfarb–Shanno) in a parallel computing environment. Our new model was benchmarked with the conventional robust planning model without considering BS. Dose–volume histograms (DVHs) of the dose assuming a fixed RBE of 1.1 and BS for tumor and organs under nominal and uncertainty scenarios were compared to assess the plan quality between the two methods.

Results: For the 10 cases, our model outperformed the conventional robust model in avoidance of high LET in OARs. At the same time, our method could achieve dose distributions and plan robustness of tumors assuming a fixed RBE of 1.1 almost the same as those of the conventional robust model.

Conclusions: Explicitly considering LET in IMPT robust treatment planning can reduce the high LET to OARs and minimize the possible toxicity of high RBE dose to OARs without sacrificing plan quality. We believe this will allow one to design and deliver safer proton therapy. [https://doi.org/10.1002/mp.12610]

Key words: biological optimization, intensity-modulated proton therapy (IMPT), linear energy transfer (LET), robust optimization

1. INTRODUCTION

Intensity-modulated proton therapy (IMPT) has the potential to enable the generation of high-quality treatment plans. By flexibly setting nonuniform intensities for different beamlets, treatment planners can achieve highly conformal dose coverage of the target and superior sparing of adjacent organs.[1,2]

Despite its advantages, IMPT has problems arising in the stage of treatment planning and delivery.[3] Among them, variable relative biological effectiveness (RBE) and plan robustness are two prominent issues. Because the dose deposition processes of photons and protons are distinct, the biological effectiveness of IMPT may differ from that of photon therapy even for the same physical dose. Consequently, RBE is often applied to calculate the actual biological effect of IMPT, with photon therapy as a reference. Currently dosimetric calculations use a constant RBE of 1.1. Although the use of a constant RBE was judged to be acceptable in passive-scattering proton therapies, this assumption resulted from the lack of biological input parameters and oversimplified the real situation, especially for IMPT.[4–7] The problem of determining RBE values is complex and involves various factors including beam radiation quality (e.g., linear energy transfer [LET]), tissue type, physical dose, and biological endpoint.[4,8] According to in vitro experimental results, the RBE value varies markedly (from 1.0 to 1.5 for IMPT) at different regions

of a proton beam. Underestimation of RBE resulting from hot spots of the LET distribution, along with the heterogeneous beamlet intensities of proton beams, could lead to unforeseen complications of organs at risk (OARs).[8,9]

Furthermore, IMPT is more sensitive to uncertainties including proton beam range and patient setup uncertainty than photon therapy.[10–13] Considering only the nominal scenario and neglecting these uncertainties may result in an overshoot or undershoot and may deteriorate the treatment quality. Various robust planning models have been proposed to consider these uncertainties and hedge against their negative influence.[14–22] In addition, LET (thus RBE) also changes under different uncertainty scenarios. This poses additional challenges to building an effective model able to avoid high RBE doses in OARs.

In heavy ion therapy, variable RBE and incorporation of variable RBE into treatment planning is the norm in heavy ion therapy for decades.[23–25] However, for proton therapy, it is relatively new. From now on, we will only focus on the variable RBE and its application in treatment planning in proton therapy. Previous studies about RBE in proton therapy can be classified into two categories. The first category is the measurement of variable RBE and its clinical impact.[4,5,26,27] These experimental studies sparked the interest in applying variable RBE to the IMPT planning especially recently. The second category is about mitigating the influence of variable RBE in treatment planning. Tilly et al.[26] applied an RBE correction method to account for variable RBE. In their work, Wilkens and Oelfke[28] integrated RBE into the inverse treatment planning of IMPT with multiple different scanning techniques.

Several models are available to calculate RBE-weighted dose.[27,29–32] However, because of the considerable uncertainties in determining the tissue-related parameters (α and β), these models may lead to inaccuracies in IMPT planning.[27] Yet exact LET can be calculated through analytical methods or Monte Carlo simulations.[33–37] In proton therapy, RBE values increase monotonically with LET, if the same dose, the same tissue, and the same biological endpoint are given.[27,38] Therefore, LET could be used as a good surrogate for indirect RBE optimization to avoid the controversy to calculate RBE from LET in proton therapy.[8,39] Several multistage methods have been developed recently to perform the LET-guided optimization (indirect RBE optimization) in IMPT treatment planning. Giantsoudi et al.[39] introduced a multicriteria optimization IMPT treatment planning system. After the initial base plans were obtained, a set of LET-related parameters were used to evaluate the biological dose distributions and combine the base plans to maximize dose-averaged LET in tumor targets while simultaneously minimizing dose-averaged LET in normal tissue structures. Fager et al.[40] applied split target planning method and multiple radiation fields to achieve higher dose-averaged LET and smaller physical dose in tumor without changing the biological effectiveness. Recently, Tseung et al.[41] used a GPU-based simulation method to demonstrate the feasibility of biological planning with variable RBE. In the work of Unkelbach et al.,[8] prioritized optimization methods were used for LET-guided optimization in IMPT treatment planning. IMPT plans were optimized first on the basis of physical doses only. In the second step, variable RBE were accounted for and plans were adjusted under certain constraints, thereby ensuring that the physical dose distribution would be minimally compromised.

In the aforementioned works, plan robustness under range and patient setup uncertainties was either neglected or implicitly dealt with by adding margins to targets. The application of margin or "planning target volume" method in proton therapy is still controversial as the dose can be distorted inside the tumor under uncertainties.[1] An ideal robust planning model of IMPT should explicitly consider the LET and the aforementioned uncertainties together.

Therefore, in this paper, we extend the LET-guided optimization methods developed in different groups[8,39,42] and propose a LET-guided robust planning model that simultaneously considers proton range and patient setup uncertainties and spares high RBE in the OARs. Our model is an extension of the model in Liu et al.,[1] which has been shown to be effective in dealing with uncertainties. Unlike the multistage optimization models mentioned above,[8,39,42] our model can find an optimal plan in a single stage using the conventional quadratic optimization. Thus, our method can be easily integrated into the current commercial treatment planning system for proton therapy such as Eclipse™ (Varian Medical Systems, Palo Alta, CA, USA). The model can minimize the high LET in OARs while maintaining almost the same tumor dose coverage and robustness in targets as those of the conventional robust model for IMPT treatment plans.

2. MATERIALS AND METHODS

2.A. Worst-case robust planning model with linear energy transfer

During IMPT, the patient receives irradiation in multiple proton beams with different incident angles. Each beam can be divided into thousands of beamlets and we used j as the index of beamlet. With k_{ij} as the physical dose deposited to voxel i by beamlet j with unit intensity (so-called influence matrix), the physical dose of voxel i D_i is calculated by $D_i = \sum_j k_{ij}\omega_j^2$. Of note, to guarantee the non-negativity, we used ω_j^2 to denote the intensity of beamlet j. We denoted the prescription dose of tumor and allowable dose to organ as $D_{0,CTV}$ and $D_{0,OAR}$.

Proton range and patient setup uncertainties can cause k_{ij} to deviate from its nominal value. To hedge against the negative influence of uncertainties, Liu et al. studied a robust model using the worst-case dose (i.e., maximum and minimum doses inside the tumor and maximum doses for normal organs assuming a fixed RBE of 1.1) in the objective function and penalized excessively high and low doses of tumors and high doses of organs.[1,43,44] In the present work, we extended the original robust model by adding a term that took into account the "biological surrogate (BS)" for each voxel in the OARs, as well as its robustness under uncertainties.

2.B. Ro(bs)

$$\min \sum_{i\in CTV}\left(p^{c}_{CTV}\left(D^{min}_{i}-D_{0,CTV}\right)^{2}+p^{h}_{CTV}\left(D^{max}_{i}-D_{0,CTV}\right)^{2}\right)+\sum_{i\in OARs}p_{OAR}\left(D^{max}_{i}-D_{0,OAR}\right)^{2}_{+}+\underline{\sum_{i\in OARs}p^{BD}_{OAR}\left(BS^{max}_{i}-BS_{0,OAR}\right)^{2}_{+}}$$

The Heavyside function $(BS^{max}_{i}-BS_{0,OAR})_{+}$ takes the value of $(BS^{max}_{i}-BS_{0,OAR})$ if $(BS^{max}_{i}-BS_{0,OAR})\geq 0$ and 0 otherwise. For targets, we constrained only the hot and cold spots based on physical dose in clinical target volume (CTV). But for OARs, we added a new term (underlined) that aimed to restrict the high *BS*. Considerable controversy exists about how to calculate RBE from LET.[8,9,40] And it has been reported that the RBE values in proton therapy increases monotonically with LET with a given endpoint, dose, and tissue type.[27,38] Therefore, LET could be used as a good surrogate for indirect RBE optimization to avoid the controversy to calculate RBE from LET in proton therapy.[8,39] Therefore, here we followed the idea proposed by Unkelbach et al.[12] to use LET as a surrogate of RBE.[8] The biological surrogate BS_i is defined as $\sum_j(1+cL_{ij})k_{ij}\omega_j^2$, where L_{ij} is the LET of beamlet j in voxel i and c is a scaling parameter.[8] c is set to be 0.04 μm/keV following the suggestion from Unkelbach et al.,[8] which yields an RBE of 1.1 in the center of a spread-out Bragg peak of 5-cm modulation and 10-cm range where the dose-averaged LET is approximately 2.5 keV/μm. The BS_i can also be expressed as $D_i + c\sum_j L_{ij}k_{ij}\omega_j^2$. Therefore, the $c\sum_j L_{ij}k_{ij}\omega_j^2$ can be seen as an extra biological effect (*xBD*) that resulted from the dose-averaged LET. p^c_{CTV}, p^h_{CTV}, p_{OAR}, and p^{BD}_{OAR} are the penalty weights for different terms. Similar to other terms, in the optimization step, the worst (maximum) BS_i among all scenarios is derived. The *BS* larger than $BS_{0,OAR}$ is penalized in the model.

By removing the underlined term we obtained a conventional robust model that did not consider biological effect of LET, as proposed in Liu et al.[1] Our new model, denoted by RO(BS), was benchmarked with this conventional model (denoted by RO). To demonstrate the importance of considering different LET in different scenarios, we also compared the new model with a benchmark that considers only nominal LET, denoted by RO(BS_0). RO(BS_0) was obtained by replacing the underlined term with $\sum_{i\in OARs}p^{BD}_{OAR}(BS^0_i-BS_{0,OAR})^2_+$, where BS^0_i represents the *BS* in the nominal scenario.

2.C. Patient data and computation settings

In this exploratory study, we tested the effectiveness of our model on 10 clinical cases: two prostate cancer, four head-and-neck cancer, and four lung cancer. For each case, we generated eight representative scenarios in addition to the

TABLE I. Comparison of tumor dose distribution assuming a fixed RBE value of 1.1. The new model RO(BS) and the conventional model RO are almost the same in quality of tumor dose coverage, homogeneity, and robustness.

		Case 1		Case 2		Case 3		Case 4		Case 5	
Index	Scenario	RO(BS)	RO	RO(BS)	RO	RO(BS)	RO	RO(BS)	RO	RO(BS)	RO
$D_{95\%}$, Gy[RBE]	Nominal	75.8	75.9	46.5	46.6	59.8	59.8	59.6	59.6	44.5	44.8
	Max	75.8	75.9	46.5	46.6	59.9	59.9	59.6	59.6	44.5	44.8
	Min	75.2	75.6	45.2	45.7	59.4	59.6	58.3	58.2	44.2	44.5
$D_{5\%}$–$D_{95\%}$, Gy[RBE]	Nominal	1.4	1	3.6	3.3	0.9	0.9	3.9	3.8	1.8	1.3
	Max	1.7	1.1	4.6	4	1.2	1.1	4.6	4.5	2	1.5
	Min	1.3	0.8	3.6	3.3	0.9	0.9	3.6	3.6	1.7	1.3
$D_{95\%}$ DVH band, Gy[RBE]		0.6	0.3	1.3	0.9	0.5	0.3	1.3	1.4	0.3	0.3
$D_{50\%}$ DVH band, Gy[RBE]		0.2	0.2	0.4	0.2	0.4	0.4	0.2	0.2	0.2	0.2
$D_{5\%}$ DVH band, Gy[RBE]		0.6	0.4	0.6	0.7	0.5	0.4	1.3	1.5	0.3	0.3
		Case 6		Case 7		Case 8		Case 9		Case 10	
		RO(BS)	RO	RO(BS)	RO	RO(BS)	RO	RO(BS)	RO	RO(BS)	RO
$D_{95\%}$, Gy[RBE]	Nominal	76.6	76.8	59.5	59.4	56.7	56.7	44.4	44.5	59.7	59.8
	Max	76.7	76.8	59.5	59.4	57.2	57.2	44.4	44.5	59.7	59.8
	Min	75.2	75.4	53.7	53.7	55.7	55.8	43.2	43.7	58	58.7
$D_{5\%}$–$D_{95\%}$, Gy[RBE]	Nominal	4.3	4.3	7.4	7.6	8.5	8.4	3.3	3.2	2.9	2.6
	Max	8	7.8	12.3	12.3	9.2	9	3.9	3.6	2.5	3.1
	Min	3.8	3.1	7.4	7.6	7.9	7.7	3.3	3.1	2.9	2.4
$D_{95\%}$ DVH band, Gy[RBE]		1.5	1.4	5.8	5.7	1.5	1.4	1.2	0.8	1.7	1.1
$D_{50\%}$ DVH band, Gy[RBE]		0.3	0.2	1.4	1.4	1.1	1.1	0.9	0.6	0.4	0.3
$D_{5\%}$ DVH band, Gy[RBE]		3.7	3.7	1.5	1.5	1.9	1.7	1	0.8	1.5	1.6

DVH, dose–volume histogram.

nominal scenario for the proton range and patient setup uncertainties. The patient setup uncertainties were simulated by shifting the isocenter of the patient in the anteroposterior (A-P), superior–inferior (S-I), and right–left (R-L) directions by 3 mm yielding six scenarios. This distance is disease-site dependent and it was set as 3 mm in this study for demonstration purposes. Range uncertainties were simulated by scaling the stopping power ratios by ±3.5% to generate two additional scenarios. The influence matrix for nominal or for each of the uncertainty scenario was calculated using a treatment planning system developed in-house.[1,45] The calculation of LET effect (L_{ij}) in each scenario was performed with an in-house fast LET calculation method based on Monte Carlo simulations. Computational settings are listed in Table A1.

2.D. Solution methods and plan evaluation

The new model RO(BS), the conventional robust model RO, and RO(BS_0) are classified as unconstrained convex programming problems. The dose volume constraints can be implemented following the method of Wu and Mohan.[46] Computation of the cases was completed in a parallel computation environment based on the L-BFGS (limited-memory Broyden–Fletcher–Goldfarb–Shanno) algorithm.[47]

To evaluate the quality of tumor dose distribution, we used $D_{95\%}$, $D_{5\%–95\%}$, and width of the dose–volume histogram (DVH) band, which displayed the envelope of all DVHs of the nine scenarios. These three parameters reflect dose coverage, dose homogeneity, and plan robustness, respectively. To

TABLE II. Comparison of biological surrogate-volume histogram indices in organs at risk for the 10 cases. Our new model RO(BS) can drastically reduce *BS* in all organs compared with RO. In comparing the results from RO(BS) and RO(BS_0), consideration of varying linear energy transfer in different uncertainty scenarios can generally further decrease the *BS* index. The unit of Gy[LET] is used here to emphasize that the values reported here are not RBE doses, but rather biological surrogates, which only have LET information.

			RO(BS)		RO		RO(BS_0)	
Case no.	Organ		Nominal	Maximum	Nominal	Maximum	Nominal	Maximum
1	Rectum	V_{25}, %	6	7	9	13	5	7
	Bladder	V_{25}, %	9	17	15	19	10	16
2	Brain stem	$D_{1\%}$, Gy[LET]	54.2	54.5	55.7	56.2	54.2	56.8
	Cord	$D_{1\%}$, Gy[LET]	11.8	18.1	23	30.9	12.6	24.2
	Oral cavity	D_{mean}, Gy[LET]	2.5	3.3	2.86	3.61	2.54	3.35
3	Brain stem	$D_{1\%}$, Gy[LET]	2.5	5.2	30.2	38.7	4.5	8.5
	Brain	$D_{1\%}$, Gy[LET]	15.7	20.9	26	30.9	17.6	22.7
	Cord	$D_{1\%}$, Gy[LET]	6.1	7.4	20.1	22.2	7.7	9.2
	Oral cavity	D_{mean}, Gy[LET]	2.73	3.28	4.13	5.02	2.89	3.53
4	Lung	V_{20}, %	10	11	11	12	10	12
		D_{mean}, Gy[LET]	5.36	6.05	6	6.72	5.5	6.2
	Heart	$D_{33\%}$, Gy[LET]	0	0	0	0	0	0
	Esophagus	$D_{33\%}$, Gy[LET]	1.2	1.8	3.4	6.5	1.4	2
	Cord	$D_{1\%}$, Gy[LET]	27.1	35.6	37.4	38.2	36.4	37
5	Lung	V_{20}, %	0.11	0.12	0.14	0.15	0.12	0.13
		D_{mean}, Gy[LET]	5.58	5.88	6.28	6.59	5.62	5.92
	Heart	$D_{33\%}$, Gy[LET]	0.2	0.3	0.3	0.5	0.2	0.3
	Esophagus	$D_{33\%}$, Gy[LET]	38.4	42.1	48.6	49.1	35.8	41.4
6	Rectum	V_{25},%	16.7	26.7	20.6	31.1	16.3	26.7
	Bladder	V_{25},%	18.4	25	19.4	26	18.1	24.6
7	Brain Stem	$D_{1\%}$, Gy[RBE]	19.1	24.6	22.2	27.2	19.8	25.3
	Brain	$D_{1\%}$, Gy[RBE]	38.7	51.8	41.5	54.4	39.4	52.8
	Cord	$D_{1\%}$, Gy[RBE]	2.9	6.3	3.1	6.8	2.9	6.5
8	Brain Stem	$D_{1\%}$, Gy[RBE]	3.1	5.9	7.6	15.3	4	7.4
	Brain	$D_{1\%}$, Gy[RBE]	45.2	52.9	71.1	75.7	43.2	53
	Cord	$D_{1\%}$, Gy[RBE]	26.4	38.2	52.4	63.9	32.9	42.8
9	Lung	V_{20}, %	14.5	14.7	14.8	15	14.5	14.8
		D_{mean}, Gy[RBE]	6.8	7	7	7.1	6.9	7
	Heart	$D_{33\%}$, Gy[RBE]	0	0	0	0	0	0
	Esophagus	$D_{33\%}$, Gy[RBE]	3.2	5.4	7.8	11.7	4.4	8.6
10	Lung	V_{20}, %	0.13	0.17	0.15	0.18	0.14	0.17
		D_{mean}, Gy[RBE]	7.7	8.8	8.6	9.8	7.8	9
	Heart	$D_{33\%}$, Gy[RBE]	0.1	0.2	0.1	0.2	0.1	0.2
	Esophagus	$D_{33\%}$, Gy[RBE]	4.7	10.7	19.9	26.4	5.5	11.5

assess the protection of OARs with biological effects due to the high LET considered, we applied the *BS*-volume histogram (BSVH) or *xBD*-volume histogram (xBDVH) (a cumulative volume histogram showing the relative volume of an organ receiving at least a certain value of *BS* or *xBD*). The xBDVH is adopted for the graphical evaluation in Figure A2. For quantitative evaluation in Table II, we chose the same indices of the BSVH as those of the dose DVH assuming a fixed RBE of 1.1 (e.g., V_{25} of rectum and $D_{1\%}$ of brain stem) as no standard is widely accepted to evaluate RBE-weighted dose. Please note that the absolute value of xBD and BS is not important, but rather the relative comparison of xBD and BS matters, which shows the better protection of OARs due to the smaller biological effects caused by high LET between different treatment planning methods.

3. RESULTS

3.A. Tumor dose distribution assuming a fixed RBE of 1.1

Table I lists the results of the 10 cases. Because multiple scenarios were considered, the table shows the nominal value and the maximum and minimum values for $D_{95\%}$ and $D_{5\%-95\%}$ among all scenarios. Band widths, which indicate plan robustness, were calculated as the difference between the maximum and the minimum value among all scenarios at $D_{95\%}$, $D_{50\%}$, and $D_{5\%}$. These parameter values of the new model RO(BD) and the conventional robust model RO are similar, and the difference is less than 1.0 Gy[RBE]. Figure A1 further illustrates the DVH curves on the basis of per-voxel maximum and minimum doses of tumor in case 2. Only a minor difference was

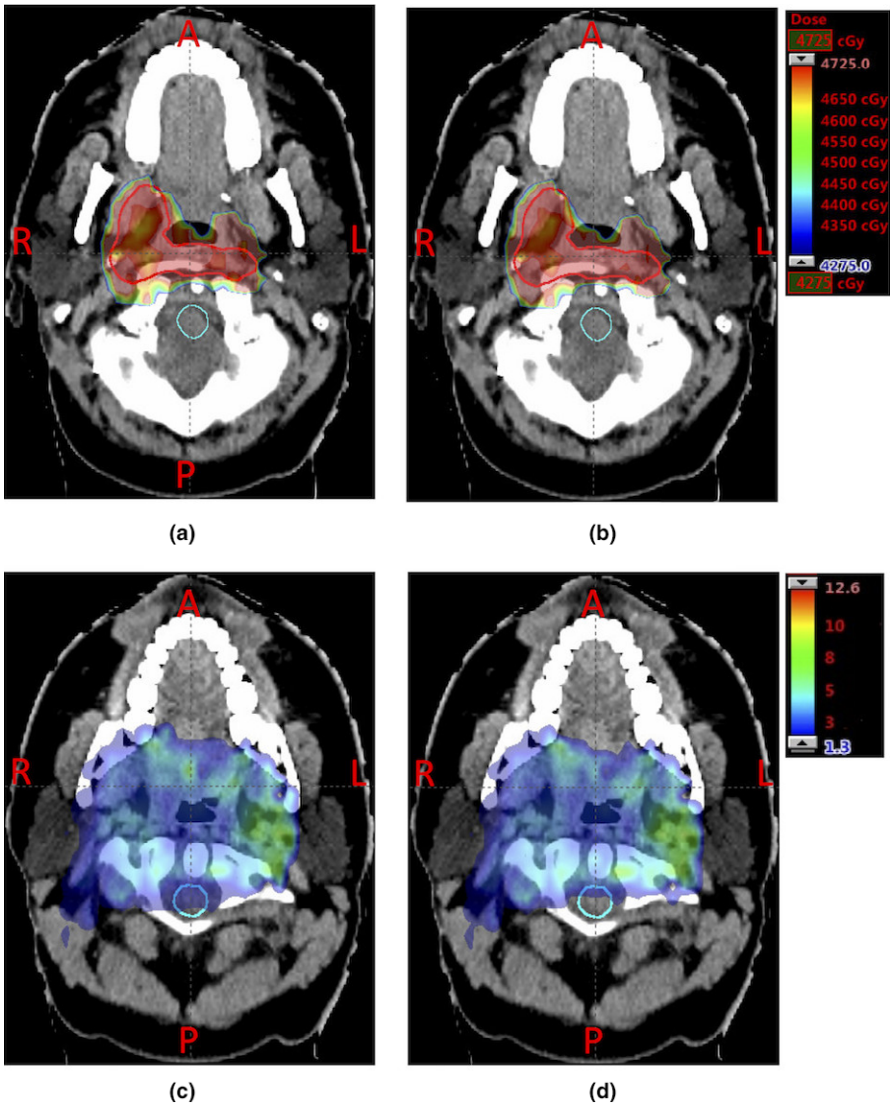

FIG. 1. Comparison of dose distribution assuming a fixed RBE of 1.1 (top row) and LET distribution (bottom row) for case 2 in the nominal scenario. (a) and (b):distribution of dose assuming a fixed RBE of 1.1. (c) and (d):distribution of the LET (unit: kev/μm). (a) and (c) are the results from the conventional model RO; (b) and (d) are the results from our new model RO(BS). Clinical target volume (CTV) and spinal cord are contoured by red (top middle enclosed area) and cyan lines (bottom enclosed area), respectively. In RO(BS), the high LET distribution in spinal cord (comparing (c) and (d)) is considerably reduced, while the physical dose distribution of the tumor is very similar. [Color figure can be viewed at wileyonlinelibrary.com]

found between the two plans, which indicates similar plan robustness of targets between the two methods.

3.B. Comparison of biological surrogate in OARs using xBDVHs and BDVHs

We defined a biological surrogate as *BS* and extra biological effects *xBD* in Section 2 to represent the biological effects because of the high LET. Figure A2 shows the xBDVHs of OARs for the first five cases. Please note again that the absolute value of xBD and BS is not important, but rather the relative comparison of xBD and BS matters, which shows the better protection of OARs due to the smaller biological effects caused by high LET between different treatment planning methods. Clearly, our new model can reduce the *xBD* in most OARs for all cases although the degree of reduction varies. Table II summarizes the *BS* of critical organs using the same indices as those of doses assuming a fixed RBE of 1.1 under the uncertainty scenarios and compares results of RO, RO(BD), and RO(BD_0) models. Both tables clearly show that the biological effects due to high LET are considerably reduced from our LET-guided robust optimization method.

Figure 1 further illustrates the difference of LET distributions of the RO(BS) and the RO for case 2 (one typical head-and-neck cancer patient). Figures 1(a) and 1(b) show the dose distribution assuming a fixed RBE of 1.1; Figures 1(c) and 1(d) show the distribution of LET. From Figure 1 (comparing (c) to (d)) we can see that the hot spot area of the LET distribution in spinal cord (with cyan contour line) is considerably reduced (highlighted by red circles in Figures 1(a) and 1(b)), while the dose distribution assuming a fixed RBE of 1.1 in tumors is very similar (comparing (a) to (b)) (highlighted by red circles in Figures 1(a) and 1(b)).

Figure 2 shows the difference of doses assuming a fixed RBE of 1.1 between the RO(BS) model and the RO model, reporting the results of the plan derived from RO(BS) minus the results of the plan from RO. To avoid high *BS* in the brainstem (yellow contour), the lower beam confines its high-intensity beamlets within its distal half and reduces the intensity of the beamlets deposited at the proximal edge of the target (red contour) when the brainstem (yellow contour) is proximal to the target. However, beamlet intensities in the upper beam parallel to the organ will increase to compensate the physical dose in the target, which leads to an increased physical dose in the red area.

3.C. Effect of considering varying LETs in different uncertainty scenarios

To demonstrate the importance of considering LET under different uncertainty scenarios, we include results from the RO(BS_0) model in Table II. By comparing the results of the three models, we find that both RO(BS) and RO(BS_0) can drastically reduce the *BS*. Generally, after including varying LETs in different uncertainty scenarios, the *BS* can be decreased further. Several exceptions exist — nominal V_{25} of rectum and worst-case V_{25} of bladder in case 1 and 6 and

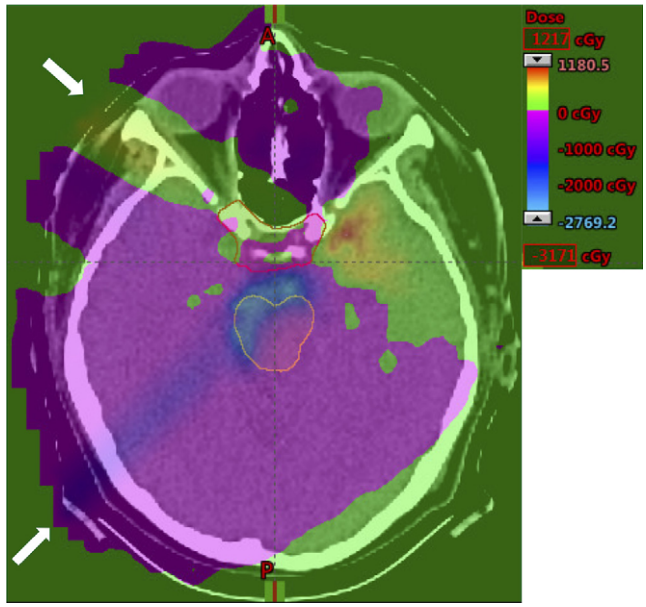

FIG. 2. Difference of doses from the results of the plan derived from the RO (BS) model minus the results of the plan derived from the RO model assuming a fixed RBE of 1.1. A representative transverse slice of case 2 under nominal scenario is shown. For two beams with their directions indicated by white arrows, the RO(BS) model clearly will reduce the intensity of beamlets of the lower beam deposited at the proximal edge of the target (red contour and top enclosed area) when brainstem (yellow contour and bottom enclosed area) is proximal to the target. This effect will lead to an decrease of physical dose (blue area and left bottom gray area) from the RO(BS) model compared with the RO model. Correspondingly, the beamlet intensities in the upper beam parallel to the brain stem will increase to compensate the physical dose in the target. This causes an increase of the physical dose in the red area (top right dark area). [Color figure can be viewed at wileyonlinelibrary.com]

nominal and worst-case $D_{33\%}$ of esophagus in case 5. The decrease is not obvious when the dose value is already small in the conventional RO models.

4. DISCUSSION

As we have emphasized in the Introduction, LET could be used as a good surrogate for indirect RBE optimization to avoid the controversy to calculate RBE from LET in proton therapy.[8,39] One may argue that the formula proposed by Unkelbach et al.[8] and used in this work can also be considered as a RBE model, which only includes LET information. However, the aim of this work was to implement a robust optimization method for IMPT to reduce high LET in OARs at no or littile cost of plan quality and plan robustness of targets. It is certainly not our intention in this work to propose a new RBE model and demonstrate its validity.

The LET is usually ignored in IMPT planning and high LET may lead to high risk of complications in OARs. Our new model simultaneously considers LET and the proton range and patient setup uncertainties so that toxic doses to organs can be minimized and tumors are still adequately covered in the face of uncertainties. On the basis of the dose-averaged LET, we defined a biological surrogate due to high LET following Unkelbach et al.[8] and added a term penalizing high *BS* of each

OAR into the IMPT robust planning model of Liu et al.[1] The new model was easy to implement and solve. All cases can be solved efficiently in a parallel computing environment.

The major concern is that introduction of new terms will compromise the tumor physical dose distribution in the original model. We investigated the influence of new terms introduced to control the distribution of LET in OARs on the quality of tumor dose distribution (Table I and Figure A1). We found that the tumor physical dose distribution from our new model was almost the same as from the conventional robust model. The robustness of tumor dose distribution was not compromised. Reduction in the *BD* does little in sacrificing the quality of tumor physical dose distribution. As demonstrated by Table I, the nominal $D_{95\%}$ change (nominal $D_{95\%}$ of the RO model minus that of the RO(BD) model as shown as (mean [min, max])) were (0.08 [−0.1, 0.3]) Gy [RBE] and the nominal $D_{5\%}$–$D_{95\%}$ change as shown as (mean [min, max]) were (−0.16[−0.5, 0]) Gy[RBE]. For robustness, the band width changes at $D_{95\%}$ as shown as (mean [min, max]) were −0.21 [−0.6, 0.1]) Gy[RBE].

Our new model drastically reduces the *xBD* because of the high LET and hence provides better overall protection to normal organs than the conventional model (Figure A2). This result is achieved primarily by reducing the mean value of *xBD* rather than the maximum *xBD*. For all cases, the middle part of the curve dropped notably while the maximums of curves varied little. This might be important for the sparing of some important parallel organs such as parotids, oral cavity, total lung, etc. The RO(BS) model and RO(BS_0) models can both greatly reduce the *BS* (Table II). This reduction is more obvious in organs receiving a large *BS* (>1.0 Gy[RBE]) under the RO planning, such as the brain stem of case 3, the cord of case 2, and the brain of case 8. The improved distribution of *BS* can decrease a patient's potential risk of organ complication.

Our RO(BS) model better protects organs against high *BS* (Fig. 2). Previous studies found that the LET increased exponentially at the end of range (at and beyond the Bragg peak).[6] Therefore, among various degenerate robust solutions, our RO(BS) model is able to find the one that reduces the intensities of beamlets deposited at the proximal edge of tumors and confines the high-intensity beamlets within its distal half. This decreases the high LET exposure in organs proximal to tumors. This observation is consistent with Grasssberger et al.[6] At the same time, to compensate the physical dose in the tumor, a beam parallel to critical structures will increase intensities of its beamlets in the target. This will further reduce high LET in critical organs as the lateral falloff of a beamlet has much lower LET compared to the distal falloff.

In this study, we explored the effect of different LETs under different uncertainty scenarios. Compared with RO(BS_0) which includes only the LET in nominal scenario, the new model RO(BS) can further reduce the *BS* in critical organs as it proactively hedges against the influence of varying LET for different uncertainty scenarios at the planning stage. Some exceptions are observed, such as the nominal V_{25} of rectum in case 1 and 6 and nominal and worst-case $D_{33\%}$ of esophagus in case 5. These exceptions can be explained by the fact that in particular challenging cases, achievement of a good protection level of one organ is contradictory with that of the other organ; hence, some organs have to be compromised.

The RO(BS) model is less effective in controlling maximum *xBD*. This problem could be solved by explicitly adding constraints, which can be implemented by following the techniques of Wu and Mohan.[46] Another alternative method is to modify the beam direction. However, incorporating new constraints or beam angle selection into treatment planning model increases the computational complexity.

5. CONCLUSION

In this work, we simultaneously included variable LET and the proton range and patient setup uncertainties into the robust IMPT planning. The plans obtained from the model were able to hedge against high LET and maintain adequate tumor coverage in the face of uncertainties. Effectively, our new model could minimize adverse consequences of the high LET exposure in OARs.

ACKNOWLEDGMENTS

This research was supported by the National Cancer Institute (NCI) Career Developmental Award K25CA168984, by Arizona Biomedical Research Commission Arizona Investigator grant, the Fraternal Order of Eagles Cancer Research Fund Career Development Award, the Lawrence W. and Marilyn W. Matteson Fund for Cancer Research, Mayo Arizona State University Seed Grant, and the Kemper Marley Foundation.

CONFLICTS OF INTEREST

The authors declare that they do not have any conflict of interest.

APPENDIX

TABLE A1 PARAMETER VALUES FOR THE 10 CASES

Case	Tumor type	Beam	Voxels
1	Prostate	1: 2,796	CTV: 303
		2: 2,788	Bladder: 651
			Rectum: 1,545
2	Head and neck	1: 5,988	CTV: 991
		2: 6,168	Brain stem: 216
		3: 6,582	Cord: 157
			Oral cavity: 1,608
3	Head and neck	1: 18,478	CTV: 1,087
		2: 14,060	Oral cavity: 1,077
			Cord: 188
			Brain stem: 195
			Brain: 12,364
4	Lung	1: 5,394	GTV: 827
		2: 7,490	Cord: 309
			Esophagus: 388
			Heart: 4,761
			Lung: 20,546
5	Lung	1: 6,780	ITV: 1,155
		2: 6,810	Lung: 26,173
		3: 7,026	Heart: 5,291
			Esophagus: 387
6	Prostate	1: 4,608	CTV: 967
		2: 4,048	Bladder: 2,776
			Rectum: 1,373
7	Head and neck	1: 2,378	CTV: 415
		2: 3,664	Brain stem: 222
		3: 3,748	Brain: 10,751
			Cord: 50
8	Head and neck	1: 11,374	CTV: 3,786
		2: 11,868	Cord: 228
		3: 2,478	Brain stem: 231
		4: 4,616	Brain: 13,066
9	Lung	1: 8,662	ITV: 1,123
		2: 4,952	Esophagus: 379
		3: 5,498	Heart: 7,085
			Lung: 24,394
10	Lung	1: 31,756	CTV: 661
		2: 37,216	Lung: 5,489
			Heart: 695
			Esophagus: 50

CTV, clinical target volume; GTV, gross tumor volume; ITV, internal target volume.

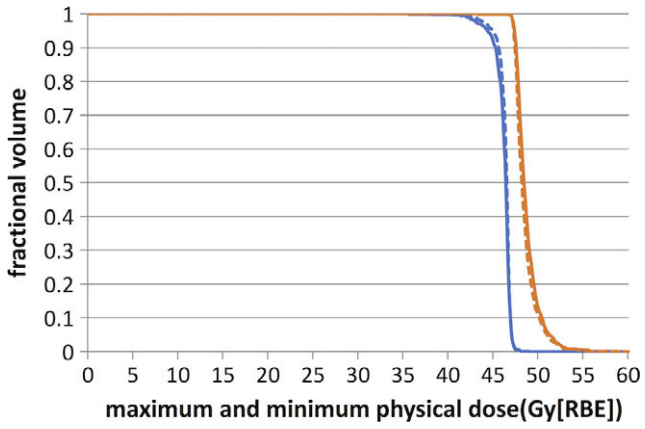

FIG. A1. Comparison of DVH curves generated by the per-voxel maximum (red and dark) and minimum (blue and gray) l doses of tumor assuming a fixed RBE of 1.1 derived from the models with and without *BS* terms for the head-and-neck cancer case. The new model RO(BS) is represented by solid curves and the conventional model RO by dashed curves. The difference between the DVH curves generated by the per-voxel maximum and minimum doses of tumor indicates plan robustness. The difference of plan quality and plan robustness is only minor between the two models. [Color figure can be viewed at wileyonlinelibrary.com]

[a]Author to whom correspondence sholuld be addressed. Electronic mail: liu.wei@mayo.edu.

REFERENCES

1. Liu W, Zhang X, Li Y, Mohan R. Robust optimization of intensity modulated proton therapy. *Med Phys*. 2012;39:1079–1091.
2. Liu W, Frank SJ, Li X, Li Y, Zhu RX, Mohan R. PTV-based IMPT optimization incorporating planning risk volumes vs robust optimization. *Med Phys*. 2013;40:021709.
3. Lim G, Cao W, Mohan R. Presented at the proceedings of the 15th asia pacific industrial engineering and management systems conference, pp 1520–1525, Jeju, Korea; 2014 (unpublished).
4. Paganetti H. Relative biological effectiveness (RBE) values for proton beam therapy. Variations as a function of biological endpoint, dose, and linear energy transfer. *Phys Med Biol*. 2014;59:R419.
5. Grassberger C, Paganetti H. Elevated LET components in clinical proton beams. *Phys Med Biol*. 2011;56:6677.
6. Grassberger C, Trofimov A, Lomax A, Paganetti H. Variations in linear energy transfer within clinical proton therapy fields and the potential for biological treatment planning. *Int J Radiat Oncol Biol Phys*. 2011;80:1559–1566.
7. Gridley DS, Pecaut MJ, Mao XW, Wroe AJ, Luo-Owen X. Biological effects of passive versus active scanning proton beams on human lung epithelial cells. *Technol Cancer Res Treat*. 2015;14:81–98.

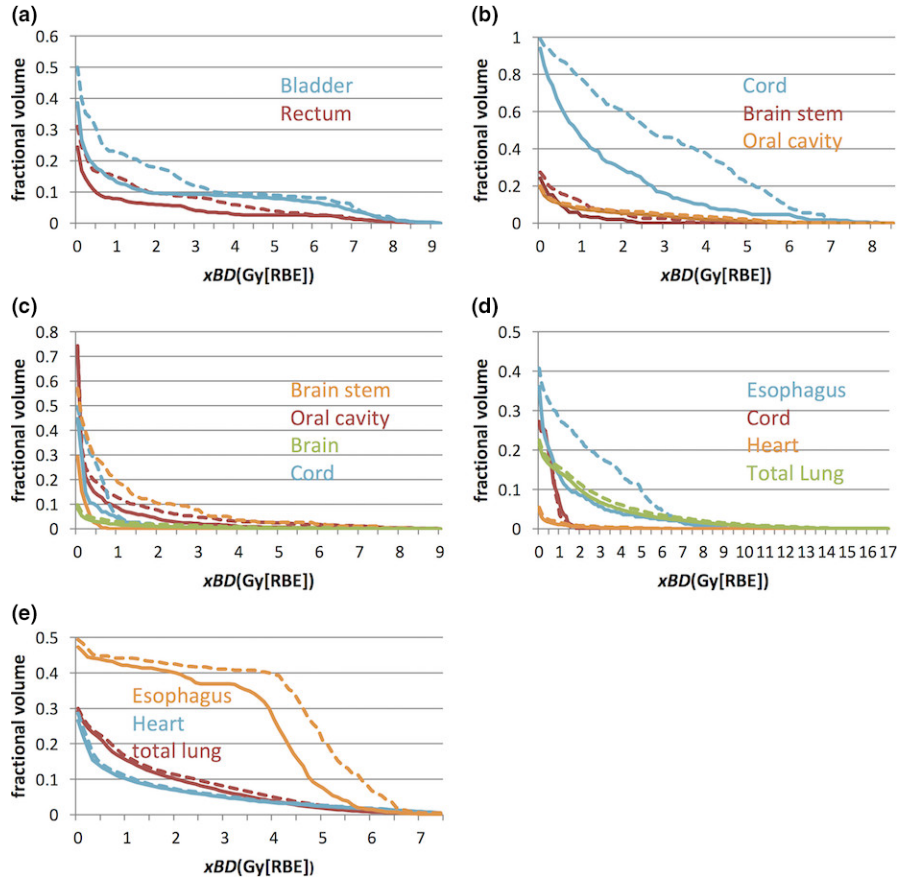

FIG. A2. The *xBD*-volume histograms of the cases 1–5 (in the nominal scenario) for RO (dashed Line) and RO(BS) (solid Line), respectively. The curves from our new robust model RO(BS) were drawn as solid lines and ones from the conventional model RO as dashed lines. The RO model can reduce *xBD*, although the degree of reduction varies from patient to patient and organ to organ. [Color figure can be viewed at wileyonlinelibrary.com]

8. Unkelbach J, Botas P, Giantsoudi D, Gorissen BL, Paganetti H. Reoptimization of intensity modulated proton therapy plans based on linear energy transfer. *Int J Radiat Oncol Biol Phys*. 2016;96:1097–1106.
9. Frese MC, Wilkens JJ, Huber PE, Jensen AD, Oelfke U, Taheri-Kadkhoda Z. Application of constant vs. variable relative biological effectiveness in treatment planning of intensity-modulated proton therapy. *Int J Radiat Oncol Biol Phys*. 2011;79:80–88.
10. Register SP, Zhang X, Mohan R, Chang JY. Proton stereotactic body radiation therapy for clinically challenging cases of centrally and superiorly located stage I non-small-cell lung cancer. *Int J Radiat Oncol Biol Phys*. 2011;80:1015–1022.
11. Kang Y, Zhang X, Chang JY, et al. 4D Proton treatment planning strategy for mobile lung tumors. *Int J Radiat Oncol Biol Phys*. 2007;67:906–914.
12. Zhang X, Li Y, Pan X, et al. Intensity-modulated proton therapy reduces the dose to normal tissue compared with intensity-modulated radiation therapy or passive scattering proton therapy and enables individualized radical radiotherapy for extensive stage IIIB non-small-cell lung cancer: a virtual clinical study. *Int J Radiat Oncol Biol Phys*. 2010;77:357–366.
13. Jiang SB, Pope C, Al Jarrah KM, Kung JH, Bortfeld T, Chen GT. An experimental investigation on intra-fractional organ motion effects in lung IMRT treatments. *Phys Med Biol*. 2003;48:1773.
14. Unkelbach J, Bortfeld T, Martin BC, Soukup M. Reducing the sensitivity of IMPT treatment plans to setup errors and range uncertainties via probabilistic treatment planning. *Med Phys*. 2009;36:149–163.
15. Unkelbach J, Chan TC, Bortfeld T. Accounting for range uncertainties in the optimization of intensity modulated proton therapy. *Phys Med Biol*. 2007;52:2755.
16. Pflugfelder D, Wilkens J, Oelfke U. Worst case optimization: a method to account for uncertainties in the optimization of intensity modulated proton therapy. *Phys Med Biol*. 2008;53:1689.
17. Fredriksson A, Forsgren A, Hårdemark B. Minimax optimization for handling range and setup uncertainties in proton therapy. *Med Phys*. 2011;38:1672–1684.
18. Fredriksson A. A characterization of robust radiation therapy treatment planning methods—from expected value to worst case optimization. *Med Phys*. 2012;39:5169–5181.
19. Liu W, Li Y, Li X, Cao W, Zhang X. Influence of robust optimization in intensity-modulated proton therapy with different dose delivery techniques. *Med Phys*. 2012;39:3089–3101.
20. Liu W, Frank SJ, Li X, et al. Effectiveness of robust optimization in intensity-modulated proton therapy planning for head and neck cancers. *Med Phys*. 2013;40:051711.
21. Liu W, Liao Z, Schild SE, et al. Impact of respiratory motion on worst-case scenario optimized intensity modulated proton therapy for lung cancers. *Pract Radiat Oncol*. 2015;5:e77–e86.
22. An Y, Liang J, Schild SE, Bues M, Liu W. Robust treatment planning with conditional value at risk chance constraints in intensity modulated proton therapy. *Med Phys*. 2017;44:28–36.
23. Jakel O, Kramer M, Karger CP, Debus J. Treatment planning for heavy ion radiotherapy: clinical implementation and application. *Phys Med Biol*. 2001;46:1101–1116.
24. Kramer M, Scholz M. Treatment planning for heavy-ion radiotherapy: calculation and optimization of biologically effective dose. *Phys Med Biol*. 2000;45:3319–3330.
25. Schardt D, Elsasser T, Schulz-Ertner D. Heavy-ion tumor therapy: physical and radiobiological benefits. *Rev Mod Phys*. 2010;82:383–425.
26. Tilly N, Johansson J, Isacsson U, et al. The influence of RBE variations in a clinical proton treatment plan for a hypopharynx cancer. *Phys Med Biol*. 2005;50:2765.
27. Carabe A, Moteabbed M, Depauw N, Schuemann J, Paganetti H. Range uncertainty in proton therapy due to variable biological effectiveness. *Phys Med Biol*. 2012;57:1159.
28. Wilkens JJ, Oelfke U. Optimization of radiobiological effects in intensity modulated proton therapy. *Med Phys*. 2005;32:455–465.
29. Wilkens J, Oelfke U. A phenomenological model for the relative biological effectiveness in therapeutic proton beams. *Phys Med Biol*. 2004;49:2811.
30. Wedenberg M, Lind BK, Hårdemark B. A model for the relative biological effectiveness of protons: the tissue specific parameter α/β of photons is a predictor for the sensitivity to LET changes. *Acta Oncol*. 2013;52:580–588.
31. McNamara AL, Schuemann J, Paganetti H. A phenomenological relative biological effectiveness (RBE) model for proton therapy based on all published in vitro cell survival data. *Phys Med Biol*. 2015;60:8399.
32. Rebecca G, Thomas F, Michael K, Michael S. Systematics of relative biological effectiveness measurements for proton radiation along the spread out Bragg peak: experimental validation of the local effect model. *Phys Med Biol*. 2017;62:890.
33. Marsolat F, De Marzi L, Pouzoulet F, Mazal A. Analytical linear energy transfer model including secondary particles: calculations along the central axis of the proton pencil beam. *Phys Med Biol*. 2016;61:740.
34. Wilkens JJ, Oelfke U. Analytical linear energy transfer calculations for proton therapy. *Med Phys*. 2003;30:806–815.
35. Sanchez-Parcerisa D, Cortés-Giraldo M, Dolney D, Kondrla M, Fager M, Carabe A. Analytical calculation of proton linear energy transfer in voxelized geometries including secondary protons. *Phys Med Biol*. 2016;61:1705.
36. Guan F, Peeler C, Bronk L, et al. Analysis of the track-and dose-averaged LET and LET spectra in proton therapy using the geant4 Monte Carlo code. *Med Phys*. 2015;42:6234–6247.
37. Romano F, Cirrone G, Cuttone G, et al. A Monte Carlo study for the calculation of the average linear energy transfer (LET) distributions for a clinical proton beam line and a radiobiological carbon ion beam line. *Phys Med Biol*. 2014;59:2863.
38. Paganetti H, Niemierko A, Ancukiewicz M, et al. Relative biological effectiveness (RBE) values for proton beam therapy. *Int J Radiat Oncol Biol Phys*. 2002;53:407–421.
39. Giantsoudi D, Grassberger C, Craft D, Niemierko A, Trofimov A, Paganetti H. Linear energy transfer-guided optimization in intensity modulated proton therapy: feasibility study and clinical potential. *Int J Radiat Oncol Biol Phys*. 2013;87:216–222.
40. Fager M, Toma-Dasu I, Kirk M, et al. Linear energy transfer painting with proton therapy: a means of reducing radiation doses with equivalent clinical effectiveness. *Int J Radiat Oncol Biol Phys*. 2015;91:1057–1064.
41. Tseung HSWC, Ma J, Kreofsky CR, Ma DJ, Beltran C. Clinically applicable monte carlo–based biological dose optimization for the treatment of head and neck cancers with spot-scanning proton therapy. *Int J Radiat Oncol Biol Phys*. 2016;95:1535–1543.
42. Ödén J, Eriksson K, Toma-Dasu I. Inclusion of a variable RBE into proton and photon plan comparison for various fractionation schedules in prostate radiation therapy. *Med Phys*. 2017;44:810–822.
43. Lomax A. Intensity modulated proton therapy and its sensitivity to treatment uncertainties 1: the potential effects of calculational uncertainties. *Phys Med Biol*. 2008;53:1027.
44. Lomax A. Intensity modulated proton therapy and its sensitivity to treatment uncertainties 2: the potential effects of inter-fraction and inter-field motions. *Phys Med Biol*. 2008;53:1043.
45. Li Y, Zhu RX, Sahoo N, Anand A, Zhang X. Beyond Gaussians: a study of single-spot modeling for scanning proton dose calculation. *Phys Med Biol*. 2012;57:983.
46. Wu Q, Mohan R. Algorithms and functionality of an intensity modulated radiotherapy optimization system. *Med Phys*. 2000;27:701–711.
47. Liu DC, Nocedal J. On the limited memory BFGS method for large scale optimization. *Math Program*. 1989;45:503–528.